Projection x-ray microscope powered by highly charged ions

R. E. Marrs, D. H. Schneider, and J. W. McDonald
Lawrence Livermore National Laboratory, Livermore, California 94551

(Received 30 June 1997; accepted for publication 1 October 1997)

Recombination of slow highly charged ions at the surface of a target foil can be used as a source of x rays for a projection x-ray microscope. In a first test of this concept, a low emittance beam of Ar^{18+} and Ar^{17+} ions from an electron beam ion trap was focused with einzel lenses to a 20 μm full width at half maximum spot on a beryllium target foil. The 3 keV x rays from radiative deexcitation of the ions were used to obtain a magnified image of an electroformed nickel mesh with 20 μm resolution by projection onto a CCD camera. Prospects for substantial improvements in resolution and intensity are discussed. © *1998 American Institute of Physics.* [S0034-6748(98)00801-6]

I. INTRODUCTION

X-ray microscopy provides information unobtainable with visible-light microscopy due to the different absorption properties of x rays and the possibility of imaging smaller structures. As the capabilities of x-ray microscopes improve, they are becoming valuable tools in biology and materials science.[1–4] Three different types of x-ray sources are presently used for x-ray microscopy: conventional x-ray tubes and other electron-beam devices,[5–9] plasma sources,[10] and synchrotron radiation.[2–4] Several different techniques have been used to obtain microscopic images with these sources.

High quality x-ray images can be obtained with synchrotron radiation, and most synchrotron radiation facilities have beam lines for x-ray microscopy. The best resolution has been obtained at low x-ray energy, particularly in the 300–500 eV ''water window'' of importance for biological studies. In a typical arrangement, the synchrotron radiation passes through a monochromator and is then focused to a small spot with a Fresnel-zone-plate condenser lens or a tapered capillary. An x-ray image is obtained by scanning a sample through the focused beam spot. Fluxes of about 10^6 photons per second at 350 eV have been focused to a 50-nm-diam spot for imaging biological samples.[3] In the same energy band, a lateral resolution of about 100 nm has been obtained with a pulsed plasma x-ray source.[10] At higher x-ray energy, a flux of 10^6 photons per second at 12.3 keV was measured through the 100 nm opening of a tapered capillary with a synchrotron-radiation source.[11]

X-ray microscopy with electron-beam-generated x rays has a long history.[12] Although these conventional ''laboratory'' x-ray sources have a much lower brilliance than synchrotron radiation sources, they are much smaller and can be located in individual research laboratories. Images are obtained either by scanning a sample through the collimated beam from a high power x-ray tube,[5–7] or by focusing an electron beam to a small x-ray-emitting spot and obtaining an x-ray image by projection.[8,9] The projection technique is the same as that used in the present work, except for the different nature of the x-ray source. Yada and Takahashi used the focused electron beam of a scanning electron microscope as an x-ray source for a projection x-ray microscope that achieved a resolution better than 0.2 μm at 1.7 keV x-ray energy.[8] At higher photon energies (6.4–7.5 keV), Rondot and Cazaux obtained 10 μm resolution with a similar arrangement;[9] two different x-ray energies were used to obtain element selectivity in the images.

In this article we introduce a laboratory x-ray microscope based on another type of x-ray source—the radiation from slow highly charged ions as they radiatively deexcite at the surface of a target foil.[13] This novel x-ray source avoids several fundamental limitations of conventional x-ray sources, suggesting that it could eventually lead to an x-ray microscope with superior performance. Results from the initial tests of a projection x-ray microscope powered by highly charged ions are reported here.

The key requirement for an x-ray microscope based on highly charged ions is an ion source with high brightness. The electron beam ion trap (EBIT)[14,15] and the related electron beam ion source (EBIS)[16] produce slow very-highly-charged ions with remarkably low emittance (on the order of 1 π mm mrad for typical beam energies), suggesting that it may be possible to focus low-energy ion beams from these sources to small spots suitable for projection x-ray microscopy. Low emittance is extremely important because the resolution of a projection x-ray microscope is determined by the size of the x-ray source, which in this case is exactly the same as the size of the focused ion spot.

Several other properties of EBIT ions make them attractive for x-ray microscopy. The radiation yield during surface recombination is very high, up to 5% or more of the total ion energy depending on the ion species and incident energy. (In comparison, the radiation yield for electrons striking the anode of an x-ray tube is on the order of 10^{-3}–10^{-4}, and anode heating is often a serious problem.) Unlike x-ray tubes, the recombination x-ray spectrum is bremsstrahlung-free and consists entirely of the characteristic line radiation of the incident ions. The range and scattering of slow highly charged ions is far less than that of electrons. In fact, radiative deexcitation occurs within a few nanometers of the target surface;[17] hence beam spreading does not limit the resolution. The x-ray energy can be selected by choosing an appropriate ion species, and energies up to 100 keV (uranium K x rays) are possible. These properties of highly-charged-ion-produced x rays encouraged us to explore the use of an EBIT at the Lawrence Livermore National Laboratory for x-ray microscopy.

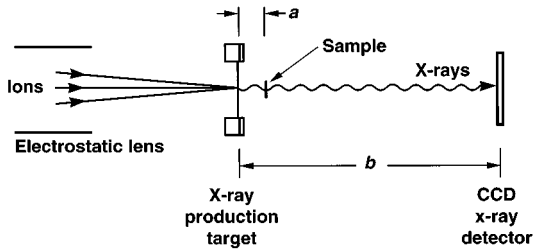

FIG. 1. Arrangement of a projection x-ray microscope using x rays from highly charged ions. Incident ions are focused to a small spot on a target foil that is transparent to the x rays produced in the recombination of the ions at the foil surface. A magnified radiograph of a sample is obtained by projection of its x-ray shadow onto a CCD camera.

II. X-RAY IMAGING

The concept of our projection x-ray microscope is illustrated in Fig. 1. Given a point source of x rays, the magnification of an x-ray image by projection is straightforward. The magnification is given by $M=b/a$, where a is the distance from the x-ray source to the sample and b is the distance from the x-ray source to the CCD. The magnification is easily adjusted by varying the sample position.

X rays are emitted isotropically from the ion recombination point. Depending on the number of vacancies and the fluorescence yield of the recombining ions, the number of x-ray photons emitted per incident ion may be more or less than one. For example, Ar^{18+} has two K-shell vacancies. Its fluorescence yield is not known precisely, but it is close to the 12% value for a K vacancy in neutral argon.[18] Ions with a nearly empty L or M shell can also be produced easily in an EBIT. In this case, multiple x-ray photons per ion are expected, particularly for heavy elements where the fluorescence yield is high. An x-ray spectrum from the recombination of Ar^{18+} and Ar^{17+} ions on a beryllium foil is shown in Fig. 2. The spectrum was obtained with a silicon photodiode detector. The 3 keV argon K x-ray peak consists of multiple satellite lines spanning an energy range of 2.96–3.30 keV for Ar^{17+} and Ar^{18+} combined.[19] Element-selective imaging is possible with our microscope by choosing incident ions whose recombination radiation is above or below selected absorption edges.

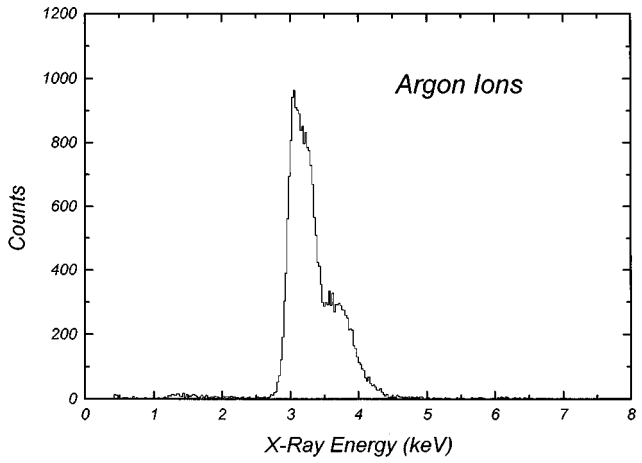

FIG. 2. X-ray spectrum of K x rays from the recombination of Ar^{18+} and Ar^{17+} ions incident on a beryllium target foil at an energy of 17.3q keV.

The resolution of a microscope is ultimately limited by the wavelength of the radiation used to form an image. In principle, the resolution of an x-ray microscope can be much better than the resolution of a visible-light microscope because x rays have much shorter wavelengths than visible light. However no x-ray microscope has come close to the wavelength limit. The resolution of the present microscope arrangement is determined entirely by the size of the focused ion spot: 20 μm for the results reported here. The contribution of diffraction to the image resolution is given by $\Delta=(\lambda a)^{1/2}$, where λ is the x-ray wavelength and a is the distance between the sample and the x-ray source. For 3 keV x rays and $a=5$ mm as in the present experiment, $\Delta=1.4$ μm. If submicron focused ion spots become available in the future, the effect of x-ray diffraction could be reduced by decreasing the sample distance.

III. ION SOURCE

In an EBIT ions are trapped within the space charge potential of a magnetically compressed electron beam. In the EBIT used for the present work, a 150 mA electron beam was compressed to a diameter of 70 μm by a 3 T magnetic field. The ions were confined to a 2 cm length of the electron beam by voltages applied to three trap electrodes. Argon ions were produced from neutral argon gas injected into the trap. Trapped ions were quickly stripped to high charge states by successive ionizing collisions with beam electrons. More detailed descriptions of the EBIT and its extracted ion beams can be found elsewhere.[14,15]

Ions were extracted from the EBIT by slowly raising the potential of the center trap electrode until the ions spilled over one of the end electrodes, which was biased at a potential of 17.3 kV. The ions were then guided by the electron beam as far as the electron collector. After passing an extraction aperture, the slightly diverging ion beam was focused onto the entrance of the x-ray microscope by an einzel lens as indicated in Fig. 3. Steerer plates were used to make small adjustments in the ion beam direction as needed.

IV. ION FOCUSING

An ion focusing column consisting of two einzel lenses and two apertures was constructed to take advantage of the low emittance of EBIT ions to produce a small focused ion spot. As shown in Fig. 3, an entrance aperture defines the initial beam size and position for the focusing column. The entrance aperture was a 0.5-mm-thick tantalum disk (to block x rays produced by ion impacts on the upstream side) with a 0.5-mm-diam hole. Each of the two einzel lenses produces a demagnified image of the entrance aperture. The amount of demagnification depends on the ion energy and the voltages applied to the einzel lenses. For the present measurements, each lens demagnified the image by a factor of roughly 5. The second lens is normally adjusted to obtain a focus at the fixed target-foil position, so it is primarily the strength of the first lens that can be varied independently to adjust the overall demagnification. Note that ions in different

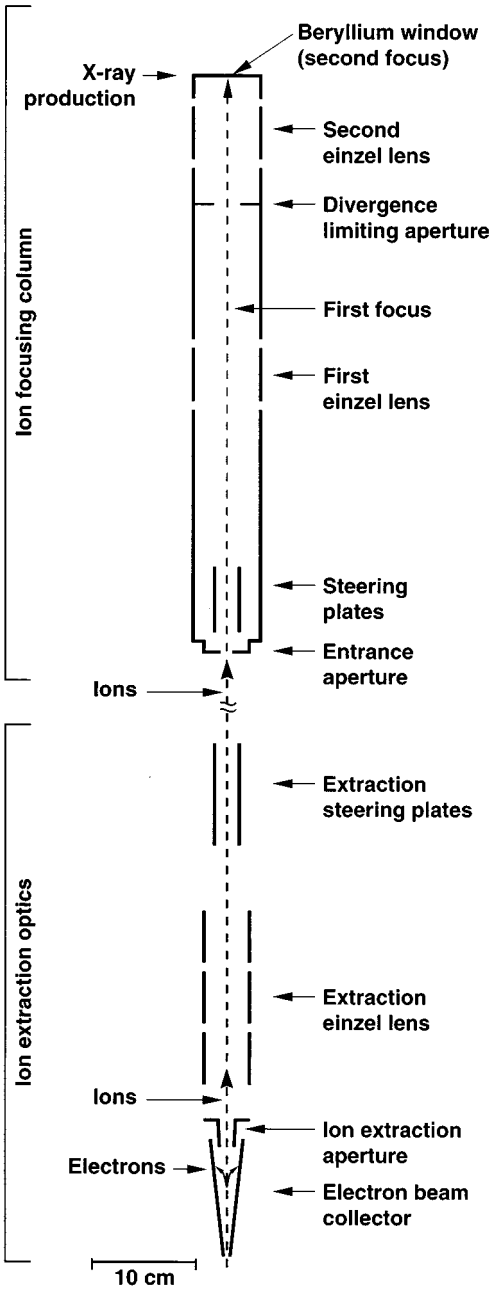

FIG. 3. Layout of the ion focusing column and the EBIT ion extraction optics.

charge states follow identical trajectories through the electrostatic lenses. Although some lower-charge-state ions are present in the beam, only Ar^{18+} and Ar^{17+} contribute to argon K x-ray production.

Ray tracing calculations show that the size of the final beam waist is limited by spherical aberrations as the strength of the einzel lenses is increased in an attempt to achieve smaller focused ion spots. The contribution of spherical aberrations to the final spot size grows as the cube of the displacement of the ions from the axis as they pass through the second lens. A 4-mm-diam aperture was placed in front of the second lens to limit the off-axis position of ions entering this lens. The effect of this aperture is to limit spherical aberrations by removing ions with a large divergence angle. Note that the initial divergence of the ions is magnified by the first einzel lens. The two apertures define the acceptance of the ion focusing column. The aperture sizes were selected so that the phase-space acceptance of the focusing column roughly matched the emittance of the ions from the source. That is, the apertures were chosen so that the beam intensity was slightly reduced.

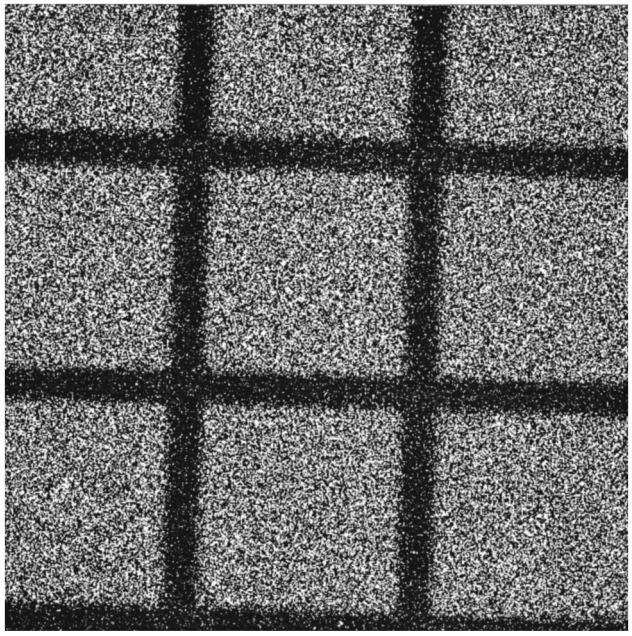

FIG. 4. Image of a nickel mesh with 3 keV x rays. The spacing of the mesh lines is 500 μm.

V. MICROSCOPE PERFORMANCE

In the present work, x rays were detected with a 512 $\times$512 pixel CCD camera. The CCD was thinned and back illuminated for sensitivity to soft x rays, and the pixel size was 25 μm. A 100-μm-thick beryllium vacuum window in front of the CCD allowed the CCD chip to operate in vacuum so that it could be cooled during image acquisition.

An electroformed nickel mesh with 70-μm-wide lines on 500 μm centers was used to test the performance of the microscope. X rays in the energy range of 3–4 keV were produced from Ar^{18+} and Ar^{17+} ions incident on a beryllium target. The x-ray spectrum is shown in Fig. 2. The nickel-mesh sample was placed in air, and a 125-μm-thick beryllium vacuum window served as the x-ray production target for the highly-charged-ion beam. The thickness of the nickel mesh was 4.7 μm, corresponding to a transmission of 8% for 3.1 keV argon $K\alpha$ x rays. As can be seen in Fig. 2, the x-ray spectrum includes a smaller flux of argon $K\beta$ x rays at 3.7 keV, for which the transmission of the nickel is 18%, but there is essentially no x-ray flux at higher energies. Hence the average x-ray transmission through the mesh is small.

The microscope was set up directly above the EBIT in a vertical orientation. The nickel mesh was located 5 mm above the x-ray source, and the CCD was 50 mm above the x-ray source, giving a magnification of $M=10$. An x-ray image of the nickel mesh from a two-hour exposure is shown in Fig. 4. The intensity of each pixel is the integral of the charge it collects from multiple x-ray events during the ex-

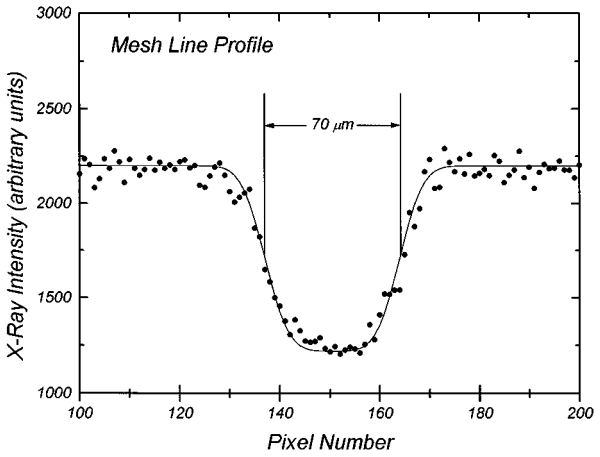

FIG. 5. Profile of one of the mesh lines in the image of Fig. 4. The solid curve is a fit with the x-ray source size adjusted to match the measured profile as explained in the text.

posure time. The noise in the image is from x-ray photon statistics and could be reduced with a longer exposure time. The contribution of electronic noise from the CCD is negligible.

The EBIT was operated with an electron beam current of 150 mA at 17.1 keV. Highly charged argon ions were produced and trapped using a 200 V axial potential well. The beryllium x-ray production target was at ground potential, so the energy of the incident argon ions was determined by the 17.3 keV potential of the top trap electrode over which the ions were extracted. Ions were extracted from the trap at 0.4 s intervals by raising the potential of the center trap electrode at a rate of 6 V/ms until it became more positive than the top electrode potential.

A. Resolution

Inspection under a visible-light microscope confirmed that the profile of the nickel-mesh lines was rectangular, so the blurring of the edges of the mesh lines in the x-ray image was used to obtain an estimate of the resolution of the x-ray microscope. The voltages on the two einzel lenses were adjusted for best resolution, resulting in values of 16.2 and 16.5 kV on the first and second lenses, respectively. These voltages were used to obtain the image of Fig. 4. Figure 5 shows a profile from one of the mesh lines of Fig. 4 obtained by averaging over 100 rows in the CCD image. Since the nickel-mesh sample was much closer to the x-ray source than the CCD, the resolution of the microscope is approximately equal to the width of the focused ion spot. If the focused ion spot has a Gaussian intensity profile with cylindrical symmetry, as expected, then each edge of a mesh line will have an error-function profile. The solid curve in Fig. 5 was calculated using a Gaussian beam profile with its width adjusted to fit the observed image. The resulting value for the diameter of the x-ray-emitting spot is 20 μm full width at half maximum (FWHM).

B. Ion emittance

The emittance and intensity of the ion beam from the EBIT source are the most important parameters determining the performance of our x-ray microscope. Although it is difficult to measure the emittance precisely, we performed some additional measurements to obtain rough estimates for the emittance and intensity of the Ar^{18+} and Ar^{17+} components of the ion beam used in the present work. Emittance is defined as $\epsilon = \pi r r'$, where r is the radius of the beam at a waist and r' is its divergence angle. The emittance is the area of the ellipse in phase space with axes of length $2r$ and $2r'$. In what follows we use an emittance that contains roughly 50% of the beam intensity. Although the beam radius is changed by the einzel lenses in the ion focusing column, the emittance is conserved. We obtained independent estimates of the beam emittance at two locations: at the entrance of the ion focusing column and at the final focused spot.

1. Measured emittance

The radius of the final focused ion spot was determined to be 10 μm as described above. Ray tracing calculations for the ion focusing column show that, for the conditions used to obtain the image of Fig. 4, ions that pass the 4 mm second aperture converge to a final focus with angles up to 70 mrad. In a run with the second aperture removed the x-ray flux increased by a factor of approximately 2, which indicates that $r' = 70$ mrad is the angle that includes roughly 50% of the beam. The 50% emittance is then 0.7 π mm mrad. This may be an underestimate of the actual EBIT emittance since some ions are also lost on the first aperture, and others are outside the 10 μm characteristic radius of the final spot.

In a separate measurement with the ion focusing column removed, a 1-mm-diam aperture was placed at the location of the entrance to the focusing column, and a beryllium target foil was placed just downstream of the aperture. The flux of Ar^{18+} and Ar^{17+} ions transmitted through the aperture was monitored by detecting 3 keV argon K x rays from the target foil with a silicon detector. The beam was centered on the aperture by applying $\leqslant 30$ V potentials to the extraction steering plates (see Fig. 3). Using the calculated beam deflection, it was found that a transverse displacement of 0.4 mm reduces the intensity of the beam transmitted through the 1 mm aperture by a factor of 2, suggesting that the beam radius is on the order of 0.4 mm or less. We obtained an independent measure of the beam size by placing a wire mesh just above the beryllium vacuum window and recording its shadow with the CCD camera. For this test the aperture was completely removed. An analysis of the wire-mesh shadow yielded a beam radius of $r \approx 0.3$ mm half width at half maximum (HWHM). Although this result was obtained during a different run period with highly charged xenon ions, beam spot sizes for argon and xenon are expected to be similar because these ions have roughly the same thermal energy per unit charge;[20] hence they follow similar trajectories.

Having determined the approximate size of the ion beam at the entrance of the ion focusing column, we now estimate the beam divergence at the same location. The 7.5 mm diameter of the EBIT extraction aperture limits the maximum size of the beam in the extraction einzel lens. This limit

corresponds to a rough upper limit of $r' < 8$ mrad for the convergence angle of ions focused at the entrance of the ion focusing column. A more accurate estimate of the ion angle can be obtained from ray tracing calculations of the ion focusing column, which show that ions with initial divergence up to 3 mrad at the entrance aperture will pass the second aperture. Combining this value of $r' = 3$ mrad with the measurements of the beam radius ($r \approx 0.3-0.4$ mm) yields an emittance of $\epsilon \approx 1.0\pi$ mm mrad.

2. Expected emittance

The expected emittance of an EBIT or EBIS can be calculated from the properties of the trapped ions. Although emittance is changed during acceleration, the normalized emittance, defined by $\epsilon_n = (v/c)\epsilon$, where v is the ion velocity, is conserved and can be related back to the temperature and volume of the trapped ions. The unnormalized emittance can then be expressed as

$$\epsilon = \pi r_0 \sqrt{kT_i/qU}, \tag{1}$$

where T_i is the temperature of the trapped ions, r_0 is the radius of their confinement volume, U is the acceleration potential, and q is the ion charge.[21] Detailed computer models of ion trapping in an EBIT predict a temperature for trapped Ar^{18+} and Ar^{17+} ions that is mainly determined by the trapping potential V_{well}. Usually, $kT_i \approx 0.1\, q\, V_{\text{well}}$,[20] a result that is supported by spectroscopic measurements of the temperature of trapped Ti^{22+} ions.[22] The ion temperature also depends on the electron beam current and other parameters, but the exponential dependence of the ion escape rate on temperature limits kT_i to a small fraction of the well depth.

The confinement radius of the trapped Ar^{18+} and Ar^{17+} ions has not been measured for the present conditions. However, since kT_i/q is close to the 14 V space charge potential at the 35 μm electron beam radius, we expect that the ion confinement radius is about the same as the electron beam radius. Hence we estimate that $r_0 \approx 35$ μm. (In a more careful calculation, which is not justified here, we would choose r_0 so that the phase space volume defined by ϵ contains exactly 50% of the ions.) Assuming $kT_i/q \approx 0.1 V_{\text{well}} = 20$ eV for the 200 V well at the beginning of the extraction ramp, the corresponding expected emittance for Ar^{18+} at 17.3 keV is $\epsilon \approx 1.2\ \pi$ mm mrad. This value could be smaller for ions extracted from a shallower well at the end of the extraction ramp. The fact that the estimates of the actual and expected emittance are similar in size suggests that if emittance growth occurs during ion extraction and separation from the electron beam, it is not a large effect.

C. Intensity

The x-ray count rate is not easily obtained from the CCD images because x rays deposit varying amounts of charge in the CCD, and some events deposit charge in more than one pixel. We used a silicon photodiode detector to measure the argon K x-ray production rate from a beryllium vacuum window located behind a 1 mm tantalum aperture. Corrections were included for x-ray attenuation in air and beryllium. The x-ray production rate was $\sim 2\times 10^5$ s^{-1} into $4\pi sr$, corresponding to 1×10^3 x-ray photons per second incident on the microscope target within the solid angle of the CCD detector. Assuming a fluorescence yield of 12%, this corresponds to an incident ion flux of $1-2\times 10^6$ s^{-1}, depending on the Ar^{18+}/Ar^{17+} ratio in the beam. This flux is comparable to a flux of 0.9×10^6 Ar^{17+} ions per second measured with a Faraday cup from an EBIT nearly identical to ours (but operating at a lower electron beam energy).[23]

It is possible to make a very rough estimate of the expected ion intensity from the operating parameters of the EBIT. Ions are confined to a length of approximately 2 cm along the electron beam. This length of beam contains 2.5×10^8 electron charges for the 150 mA, 17.1 keV beam used in the present work. If roughly 20% of the electron space charge is neutralized by argon ions, and roughly 1/2 of the argon-ion charge is in the 18+ and 17+ charge states after 0.4 s of ion influx and stripping,[20] then the trap contains 1.4×10^6 Ar^{18+} and Ar^{17+} ions. Dumping the trap every 0.4 s as in the present measurements would yield an average $Ar^{18+}+Ar^{17+}$ flux of 3.5×10^6 s^{-1}. Although this estimate of the expected ion flux is imprecise, its approximate consistency with the measured x-ray intensity suggests that the efficiency for extracting Ar^{18+} and Ar^{17+} ions and focusing them through a small aperture is good.

It should be noted that highly charged argon ions are a very common beam from EBIS devices, for which up to 10^{10} extracted positive charges per second have been reported,[16] a value two orders of magnitude larger than the flux obtained from our EBIT. Since the emittance of an EBIS is expected to be similar to that of an EBIT, these devices could become a bright source for a highly-charged-ion-based projection x-ray microscope.

VI. DISCUSSION

We have demonstrated a projection x-ray microscope using x rays from the radiative deexcitation of slow highly charged ions at a target surface. In the initial tests reported here, a resolution of 20 μm was achieved with 3 keV x rays. Yada and Takahashi have demonstrated that a resolution of better than 0.2 μm can be achieved in projection x-ray microscopy.[8] In their work, x rays were produced by focusing the electron beam of a scanning electron microscope onto a thin target foil. Different target foils and electron beam energies were investigated with regard to electron beam spreading and target heating. The resolution was limited primarily by diffraction [$\Delta = (\lambda a)^{1/2}$] and by electron beam spreading in the target. Reduction of the spot size of the highly-charged-ion beam would allow the resolution of our x-ray microscope to be reduced to the diffraction limit because spreading of the highly-charged-ion beam in the target is negligible. Target heating is not expected to limit the x-ray intensity for slow highly-charged-ion beams because their x-ray production efficiency is greater than that of electron beams.

The emittance and intensity of the highly-charged-ion beam are key parameters for the performance of our x-ray microscope. Measured values of the emittance and intensity

of the ion beam used in the present work are roughly consistent with estimates based on the properties of the source. Dramatic improvements in the highly-charged-ion-based x-ray microscope are expected to follow from improvements in the ion source. EBIT and EBIS devices with a 1000 fold increase in ion flux compared to the device used in the present work have been proposed.[24,25] Even without anticipated improvements in the ion emittance, the size of the focused ion spot could be reduced by collimation of a more intense ion beam. This is a common practice with conventional focused ion beams. We did not use a large amount of collimation with our present ion source because the image acquisition rate would have been too low. A 1000-fold increase in the present incident x-ray flux of 1×10^3 photons per second would make the flux equal to that used for scanning x-ray microscopy at the National Synchrotron Light Source (at 350 eV),[3] and at the Cornell High Energy Synchrotron Source (at 12.3 keV).[11] However the spatial resolution of the synchrotron-based microscopes is much better than the resolution obtained in the present work.

Finally, we note that the focused ion beam of 20 μm FWHM produced in the present work is, to our knowledge, the smallest ever achieved for slow highly charged ions.

ACKNOWLEDGMENTS

The authors thank E. Magee for his skillful construction of the ion focusing column. They acknowledge helpful conversations and assistance from A. V. Barnes and B. Beck. This work was performed under the auspices of the U. S. Department of Energy by Lawrence Livermore National Laboratory under Contract No. W-7405-Eng-48.

[1] M. R. Howells, J. Kirz, and D. Sayre, Sci. Am. **264**, 88 (1991).
[2] D. Sayre and H. N. Chapman, Acta. Crystallogr. A **51**, 237 (1995).
[3] J. Kirz, C. Jacobson, and M. Howells, Q. Rev. Biophys. **28**, 33 (1995).
[4] C. Kunz, Phys. Scr. **T61**, 19 (1996).
[5] A. Attaelmanan, S. Larsson, A. Rindby, P. Voglis, and A. Kuczumow, Rev. Sci. Instrum. **65**, 7 (1994).
[6] D. A. Carpenter, M. A. Taylor, and R. L. Lawson, J. Trace and Microprobe Techniques **13**, 141 (1995).
[7] N. Yamamoto, Rev. Sci. Instrum. **67**, 3051 (1996).
[8] K. Yada and S. Takahashi, in *X-Ray Microscopy II*, edited by D. Sayre, M. Howells, J. Kirz, and H. Rarback (Springer, New York, 1988), p. 323; J. Electron Microsc. **38**, 321 (1989).
[9] S. Rondot and J. Cazaux, Rev. Sci. Instrum. **68**, 1787 (1997).
[10] R. Lebert, W. Neff, and D. Rothweiler, J. X-Ray Sci. Technol. **6**, 107 (1996).
[11] D. H. Bilderback and D. J. Thiel, Rev. Sci. Instrum. **66**, 2059 (1995).
[12] V. E. Cosslett and W. C. Nixon, Nature (London) **168**, 24 (1951).
[13] D. H. G. Schneider and M. A. Briere, Phys. Scr. **53**, 228 (1996).
[14] R. E. Marrs, in *Experimental Methods in the Physical Sciences Volume 29A*, edited by F. B. Dunning and R. G. Hulet (Academic, San Diego, 1995), p. 391.
[15] D. Schneider, M. W. Clark, B. M. Penetrante, J. McDonald, D. DeWitt, and J. N. Bardsley, Phys. Rev. A **44**, 3119 (1991).
[16] E. D. Donets, in *The Physics and Technology of Ion Sources*, edited by I. G. Brown (Wiley, New York, 1989), p. 245.
[17] T. Schenkel, M. A. Briere, H. Schmidt-Böcking, K. Bethge, and D. H. Schneider, Phys. Rev. Lett. **78**, 2481 (1997).
[18] J. P. Briand, B. d'Etat-Ban, D. Schneider, M. A. Briere, V. Decaux, J. W. McDonald, and S. Bardin, Phys. Rev. A **53**, 2194 (1996).
[19] J. P. Briand, L. de Billy, P. Charles, S. Essabaa, P. Briand, R. Geller, J. P. Desclaux, S. Bliman, and C. Ristori, Phys. Rev. A **43**, 565 (1991); Phys. Rev. Lett. **65**, 159 (1990).
[20] B. M. Penetrante, J. N. Bardsley, D. DeWitt, M. Clark, and D. Schneider, Phys. Rev. A **43**, 4861 (1991).
[21] R. Keller, in *The Physics and Technology of Ion Sources*, edited by I. G. Brown (Wiley, New York, 1989), p. 23.
[22] P. Beiersdorfer, in *X-Ray and Inner-Shell Processes*, edited by R. L. Johnson, H. Schmidt-Böcking, and B. F. Sonntag, AIP Conf. Proc. No. 389 (AIP Press, New York, 1997), p. 121.
[23] L. P. Ratliff, E. W. Bell, D. C. Parks, A. I. Pikin, and J. D. Gillaspy, Rev. Sci. Instrum. **68**, 1998 (1997).
[24] E. Beebe, J. Alessi, A. Hershcovitch, A. Kponou, K. Prelec, and R. W. Schmieder, Rev. Sci. Instrum. **67**, 878 (1996).
[25] R. E. Marrs and D. H. Schneider (unpublished).